Original Article

New hybrid NSGA-III&SPEA/R to multi-object optimization in a half-car dynamic model

Dinh-Nam Dao[1,2] (ID) and Li-Xin Guo[1]

Abstract
In this article, we conducted a new hybrid method between Non-dominated Sorting Genetic Algorithm II (NSGA-III) and SPEA/R (HNSGA-III&SPEA/R). This method is implemented to find the optimal values of the powertrain mount system stiffness parameters. This is the task of finding multi-objective optimization involving six simultaneous optimization goals: mean square acceleration and mean square displacement of the powertrain mount system. A hybrid HNSGA-III&SPEA/R has proposed with the integration of Strength Pareto evolutionary algorithm-based reference direction for Multi-objective (SPEA/R) and Many-objective optimization genetic algorithm (NSGA-III). Several benchmark functions are tested, and results reveal that the HNSGA-III&SPEA/R is more efficient than the typical SPEA/R and NSGA-III. Powertrain mount system stiffness parameters optimization with HNSGA-III&SPEA/R is simulated. It proved the potential of the HNSGA-III&SPEA/R for powertrain mount system stiffness parameter optimization problem.

Introduction

The vehicle power system includes engine, transmission, and clutch. This is not only the power supply for the car, but it is also the part that causes the main vibration in the car. Therefore, the engine mount is usually installed between the power source system and the car body to limit vibration from the power system to the chassis.[1] The system consists of mounts, and power source system is a vehicle power system. Figure 1 is the principle diagram of the half-car dynamic model; in this model, the mounts play an important role. Good power source system mounts will improve the performance of noise, vibration, and harshness (NVH) of the vehicle while extending the life of the engine and related parts.[2,3] Engine mounts can be categorized according to the characteristics of the ability to control mounts. It includes passive mounts, active mounts, and semi-active mounts. Rubber mounts are the most widely used engine mounts for their low cost and simple structure. The mounts need to be designed with the parameters of the mounts to match their stiffnesses. In order to reduce the vibration of the engine to the elastic substrate and to reduce the unwanted effects of stimuli from the road,

the wheel acts on the body of the vehicle, the mounts should have the appropriate stiffness. Therefore, an important task in designing the power source system mounting system is to calculate the optimal stiffness parameters for the power source system mounting system. This is a multi-object optimization issue.

In recent years, some researchers have researched in this area. They have given different ways and techniques, among them, presented in an overview and guidelines.[4] Deb et al.[5] published the Non-dominated Sorting Genetic Algorithm II (NSGA-II) algorithm and so far, several variants and applications for NSGA-II have been developed by Chang and Chang.[6–8] Kalyanmoy and Jain[9] applied MONGA-II to a number

---

[1]School of Mechanical Engineering and Automation, Northeastern University, Shenyang, China
[2]Control Technology College, Le Quy Don Technical University, Hanoi, Vietnam

Corresponding author:
Dinh-Nam Dao, School of Mechanical Engineering and Automation, Northeastern University, Shenyang 110819, China.
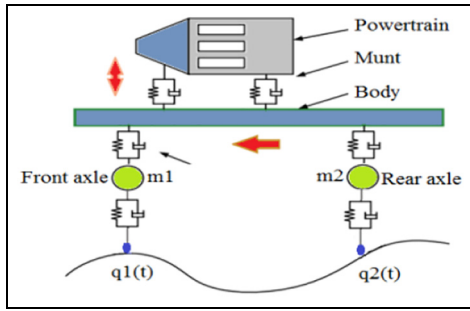Email: daodinhnambk@gmail.com

Figure 1. The half-car dynamic model.

of many-objective test problems. Deb and Jain[10] published the NSGA-III algorithm based on the NSGA-II algorithm, by changing some of the selection mechanisms. NSGA-III algorithm has been tested in multi-objective optimization.

In addition, SPEA2 algorithm is an extension of SPEA's (Strength Pareto evolutionary algorithm) multi-objective evolution optimization algorithm. This algorithm uses a mechanism such as k-Recent Neighbor (kNN) and a specialized ranking system to sort individuals of a population and choose individuals of the population in the next cycle. This is a combination of the current population and the population created by genetic operators (mutations and cross-exchanges). SPEA2 is a widely used and applied algorithm for handling real-world scientific and technical applications. There are also some researchers on this algorithm: Kim et al.[11] improved the SPEA2 algorithm to improve its searchability. E Zitzler et al.[12] published a SPEA2 algorithm: this used the increase in the power of multi-objective optimization. Borisevic and Bartlett[13] have applied this algorithm to get an optimal safety system design. Hiroyuki Mori and Hiroki Kakuta[14] proposed a new method to assess probability reliability with multi-target super therapy (MOMH) in the smart grid. De Tommasi et al.[15] studied RF circuit blocks from alternative models and normal boundary intersection (NBI) method, SPEA2 algorithm for multi-objective optimization. Sokratis Sofianopoulos[16] proposed SPEA2 algorithm for optimization in a machine translation system. F Zhao et al.[17] proposed a method to optimize adaptive selection evolutionary operators (AOSPEA) with SPEA2 algorithm. Hamida et al.[18] proposed the Pareto Strength (SPEA2) Evolution Algorithm for the Economic/Environmental Power Distribution. Jiang and Yang[19] published a SPEA/R algorithm, it is a significant extension of the early SPEA algorithm to optimize multiple goals. It applies the advantages of SPEA2's physical assignment in quantifying solutions—diversity and convergence—in one method. It is appropriate to replace the most time-consuming density estimator with an algorithm based on the reference direction. Their proposed exercise duties also take into account the convergence of both local and global.

Recently, new optimization algorithms are proposed.[20–27] However, each algorithm has advantages and disadvantages, precisely because no algorithm can solve all optimization problems correctly. Therefore, new hybrid algorithms should be proposed to be able to solve new problems that have not been resolved before and/or have better accuracy than existing techniques.

Some methods of hybridization of optimal algorithms have been developed recently: Jeong et al.[28] published the Hybrid Algorithm between genetic algorithm (GA) and particle swarm optimization (PSO) for Optimizing real-world design. Premalatha et al.[21] published a hybrid algorithm between PSO and GA for Global Maximization. Hong-bin Bai[29] proposed a way to optimize multi-target particles based on extreme optimization with variable and inertial inertia mutations (HM-TVWF-MOEPSO) to enhance the effectiveness of the algorithm while performing some problems in multi-target particle optimization. A hybrid method is proposed to combine the simple method of Nelder-Mead with the non-dominance sequencing method of NSGA-II algorithm. Pourtakdoust and Zandavi[30] have published a method to evaluate the performance of new hybrid methods. Multi-variable technical optimization issues can be handled by Pareto solutions and optimized multiple times until satisfactory results are obtained and these have been published in Guang Yang et al.[31] E Rashidi et al.[32] published an independent parallel genetic hybridization method. Thus, most published hybrid algorithms have more advantages. This hybridization has overcome the limitations of each optimization algorithm. This proves that this is one of the techniques that need to be studied in optimizing many goals.

In this paper, a new hybrid method has been proposed to find the Pareto optimization front for multi-purpose problems. This is a combination of SPEA/R algorithm and NSGA-III algorithm to find out the best Pareto-optimal front of powertrain mount system stiffness parameter. The effectiveness of the new algorithm is expressed through a number of complex benchmarking functions and for powertrain mount system stiffness parameter optimization problem with four-objective optimization in two-dimensional model.

This article is presented as follows: the "Structure" section presents hybrid HNSGA-III&SPEA/R method and computational experimentation with several benchmark functions. The section "Vibration characteristic of the half-car dynamic model" describes the system vibration characteristics of the dynamic cluster on the vehicle and simulation results of application HNSGA-III&SPEA/R method to stiffness parameter optimization of mounts system. The final section is a conclusion.

Structure

Genetic algorithm NSGA-III

Deb and Jain[10] improved the NSGA-II gene algorithm into algorithm NSGA-III. The NSGA-III algorithm is described in the flowchart of NSGA-III shown in Figure 2.
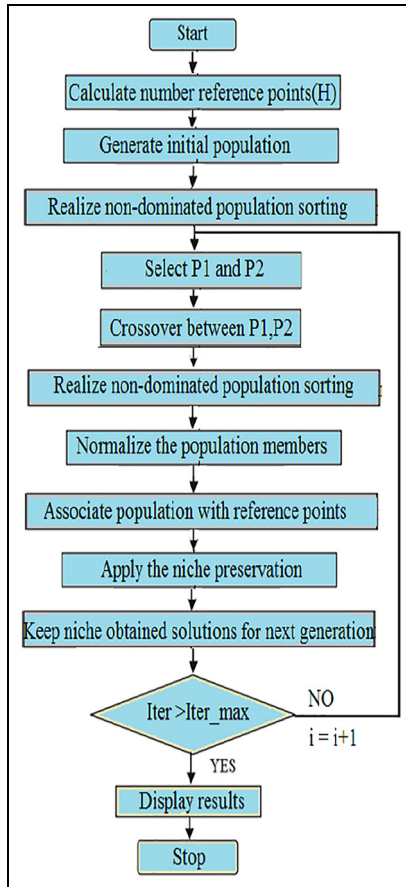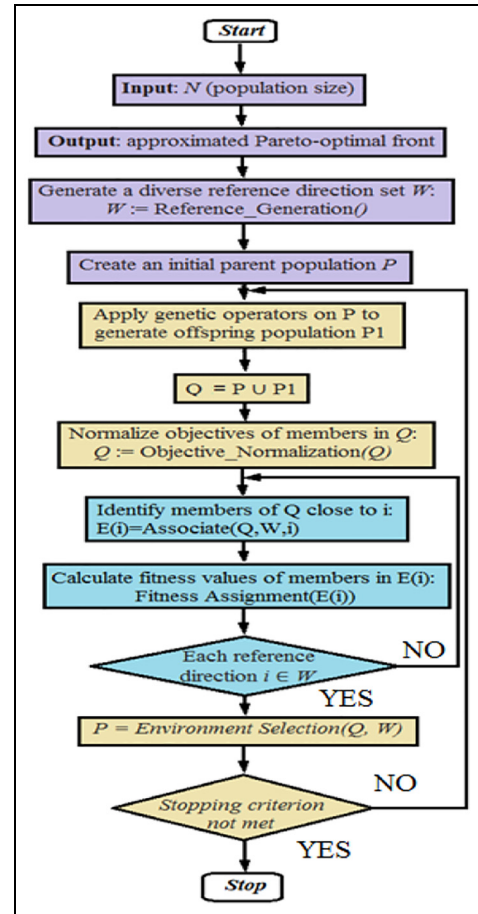
Figure 2. Flowchart of NSGA-III.

Figure 3. Flowchart of SPEA/R.
SPEA/R: Strength Pareto evolutionary algorithm.

SPEA/R algorithm

The SPEA/R algorithm has been published by Shouyong et al. (2017). The SPEA/R algorithm is shown in the diagram of SPEA/R as shown in Figure 3.

Hybrid NSGA-III and SPEA/R (HNSGA-III&SPEA/R)

Evolutionary algorithms have different strengths and weaknesses. So to handle complex problems, we often think of integrating different algorithms. In the field of research, consolidate different methods of evolution or optimization algorithms into a single algorithm. More efficient hybrid algorithms can exchange each other's strengths, all shown in the results indicating that. It can be processed in parallel to enhance exploration and exploitation. Therefore, it can have higher results than single algorithms. Use-based approaches to population use different techniques to explore the search space and when they are combined, it will advance the trade-off between exploration and exploitation tasks to converge solutions. This hybrid method has acquired the strengths of both algorithms, which are fast convergence capabilities in NSGA-III and SPEA/R diverse search capabilities, thus reducing computation time and a result of Pareto front set is more accurate than the above two methods.

HNSGA-III&SPEA/R hybrid approach. HNSGA-III&SPEA/R are implemented in parallel hybridization. That is, the original population will be both NSGA-III and SPEA/R simultaneously generated. After that, two separate populations will be mixed together. The new population after the mix will be both algorithms used as their own population to perform evaluation fitness function calculations for the evolution of each algorithm. To the next generation, the new population that is created by the two algorithms is mixed together to form a common population. The process repeats until the evolutionary termination condition is complete.

A flowchart of HNSGA-III&SPEA/R is shown in Figure 4.

Computational experimentation with several benchmark functions

For accurate and intuitive evaluation, we have selected five typical standard functions to evaluate and compare between algorithms. The three standard functions UF2, UF4, and UF5 are functions to evaluate two optimal objects simultaneously; UF8 and UF10 are functions for evaluating three optimal objects simultaneously. These are very famous standard functions and have
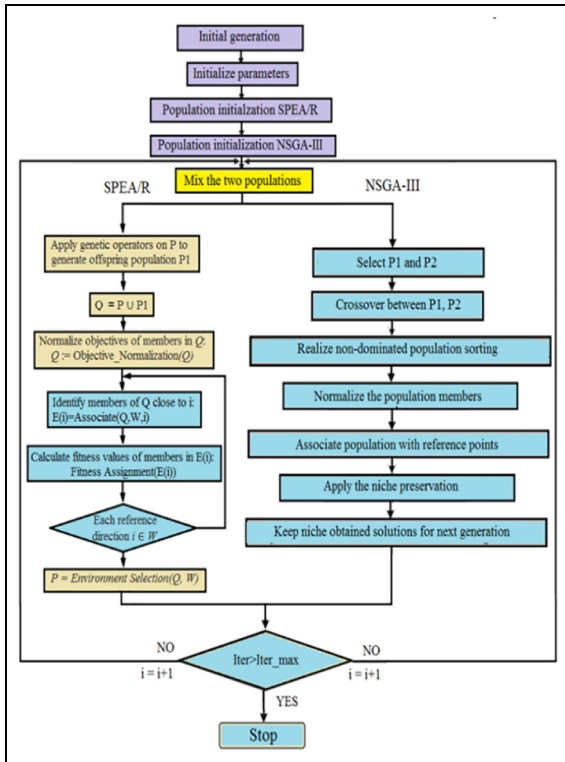
Figure 4. Flowchart of HNSGA-III&SPEA/R.
SPEA/R: Strength Pareto evolutionary algorithm.

The pseudo code of the proposed algorithm:
Initialize parameters for NSGA-III and SPEA/R.
SPEA/R: Swarm population initialization.
NSGA-III: GA population initialization.
While travel not completed.
  Mix the two populations.
  SPEA/R algorithm.
While conditions stop not responding do
  Use genetic elements on P to produce the female population P
  $Q = P \cup P$
  Assigning members' goals in Q:
  $Q = Objective\_ Assigning (Q)$
For each reference direction, $i \in W$ do
  Assign personal of Q close to i:
  $E(i) = Associate(Q, W, i)$
  Determine the physical value of personal in $E(i)$:
  Fitness_ Production $(E(i))$
End for
  P = choose the environment (Q, W)
End while.
  NSGA-III algorithm.
While evolution not completed.
  Assign two parents $P1$ and $P2$ using the tournament method.
  Assign the crossover between $P1$ and $P2$ with a probability Pc.
  Recognize the unclassified population classification.
  Normalization of population individuals.
  Linking individuals population with reference points.
  Specify appropriate storage (access).
  Keep the appropriate solutions obtained for the next generation.
  End while.
End while.

been widely used in the evaluation of optimal target optimization.

Result number: Performance of HNSGA-III&SPEA/R is proved by the five standard functions announced in CEC 2009,[33] as in Table 1. Results are evaluated with methods of NSGA-III and Multi-objective SPEA/R, for Inverted Generational Distance (IGD) of Schott.[34] Standards are used to measure the convergence, number, and corresponding coverage. IGD is calculated as follows

$$IGD = \frac{\sqrt{\sum_{i=1}^{N} d_i^2}}{N} \quad (1)$$

Here, N is the number of real Pareto-optimal front set and d_i shows the Euclidean distance between the correct ith Pareto-optimal front set and the cabinet to obtain Pareto-optimal front set. $IGD = 0$ proved that all members of the non-dominant set are in the real Pareto Front. In addition to using performance data, the best Pareto optimization solution set by HNSGA-III&SPEA/R on both parameter space and search space is shown in Figure 5 (UF1, UF4, UF5). These figures clearly show the performance of HNSGA-III&SPEA/R compared to the true Pareto front. For comparison and evaluation, these methods were run 20 times for test problems. The statistical results of 20 runs and the parameters of the methods are shown in Tables 2–4. The statistical results of the method for

IGD are presented in Table 5. Hybrid methods (HNSGA-III&SPEA/R) have been demonstrated on all statistics for two-goal test problems, that is, expressed through the IGD parameter. The performance of the accuracy and convergence of the method is reflected in the IGD index. Therefore, it has been shown that the proposed HNSGA-III&SPEA/R method can provide outstanding convergence on the two target benchmarks. Pareto-optimal solution of HNSGA-III&SPEA/R on the three target benchmarks is also described in Figure 5 (UF8, UF10).

The Pareto front result is presented in Figure 5. Numerical results have shown that the HNSGA-III&SPEA/R method has higher accuracy for benchmarking functions with two objectives related to convergence and coverage. However, for some tri-objective functions, the three targets are standard; although the proposed method shows higher convergence, it has higher coverage compared to NSGA-III and SPEA/R methods. Therefore, we can confirm that the HNSGA-III & SPEA/R method has advantages over the NSGA-III and SPEA/R methods, which are the higher convergence and coverage characteristics. In addition, in most cases, the results of HNSGA-III & SPEA/R are better than that of NSGA-III and SPEA/R. Therefore, the HNSGA-III&SPEA/R method has better results and is more accurate than the other two

Table 1. Benchmark functions for test multi-objective optimization.

Mathematics formulation	Mathematics formulation	Mathematics formulation
UF2	UF4	UF5

UF2

$$f_1 = x_1 + \frac{2}{|J_1|}\sum_{j\in J_1} y_j^2$$

$$f_2 = 1 - \sqrt{x} + \frac{2}{|J_2|}\sum_{j\in J_2} y_j^2$$

$$y_j = \begin{cases} x_j = \left[0.3x_1^2\cos\left(24\pi x_1 + \frac{4j\pi}{n}\right) + 0.6x_1\right]\sin\left(6\pi x_1 + \frac{j\pi}{n}\right) & \text{if } j\in J_1 \\ x_j = \left[0.3x_1^2\cos\left(24\pi x_1 + \frac{4j\pi}{n}\right) + 0.6x_1\right]\sin\left(6\pi x_1 + \frac{j\pi}{n}\right) & \text{if } j\in J_2 \end{cases}$$

$J_1 = \{j|j \text{ is odd and } 2 \leq j \leq n\};$
$J_2 = \{j|j \text{ is even and } 2 \leq j \leq n\};$

UF8

$$f_1 = \cos(0.5x_1\pi)\cos(0.5x_2\pi) + \frac{2}{|J_1|}\sum_{j\in J_1}\left(x_j - 2x_2\sin\left(2\pi x_1 + \frac{j\pi}{n}\right)\right)^2$$

$$f_2 = \cos(0.5x_1\pi)\cos(0.5x_2\pi) + \frac{2}{|J_2|}\sum_{j\in J_2}\left(x_j - 2x_2\sin\left(2\pi x_1 + \frac{j\pi}{n}\right)\right)^2$$

$$f_3 = \sin(0.5x_1\pi) + \frac{2}{|J_3|}\sum_{j\in J_3}\left(x_j - 2x_2\sin\left(2\pi x_1 + \frac{j\pi}{n}\right)\right)^2$$

$J_1, J_2,$ and J_3 are the same as those of UF10

UF4

$$f_1 = x_1 + \frac{2}{|J_1|}\sum_{j\in J_1} h(y_j)$$

$$f_2 = 1 - x_2 + \frac{2}{|J_2|}\sum_{j\in J_2} h(y_j)$$

$$y_j = x_j - \sin\left(6\pi x_1 + \frac{j\pi}{n}\right)$$

$j = 2, 3, ..., n$

$$h(t) = \frac{|t|}{1 + e^{2|t|}}$$

J_1 and J_2 are the same as those of UF2
UF10

$$f_1 = \cos(0.5x_1\pi)\cos(0.5x_2\pi) + \frac{2}{|J_1|}\sum_{j\in J_1}\left(4y_j - \cos(8\pi y_j + 1)\right)$$

$$f_2 = \cos(0.5x_1\pi)\cos(0.5x_2\pi) + \frac{2}{|J_1|}\sum_{j\in J_2}\left(4y_j - \cos(8\pi y_j + 1)\right)$$

$$f_3 = \cos(0.5x_1\pi) + \frac{2}{|J_3|}\sum_{j\in J_3}\left(4y_j - \cos(8\pi y_j + 1)\right)$$

$J_1 = \{j|3 \leq j \leq n \text{ and } j-1 \text{ is a multiplication of 3}\}$
$J_2 = \{j|3 \leq j \leq n \text{ and } j-2 \text{ is a multiplication of 3}\}$
$J_3 = \{j|3 \leq j \leq n \text{ and } j-3 \text{ is a multiplication of 3}\}$

UF5

$$f_1 = x_1 + \left(\frac{1}{2N} + \varepsilon\right)|\sin(2N\pi x_1)| + \frac{2}{|J_1|}\sum_{j\in J_1} h(y_j)$$

$$f_2 = 1 - x_1 + \left(\frac{1}{2N} + \varepsilon\right)|\sin(2N\pi x_1)| + \frac{2}{|J_2|}\sum_{j\in J_2} h(y_j)$$

$$y_j = x_j - \sin\left(6\pi x_1 + \frac{j\pi}{n}\right)$$

$j = 2, 3, ..., 4$

$$h(t) = 2t^2 - \cos(4\pi t) + 1$$

J_1 and J_2 are the same as those of UF2, $\delta > 0$.

Table 2. NSGA-III algorithm parameters.

Maximum number of iterations	MaxIt = 10,000	Number of parents (offsprings)	nCrossover = 2 × round(pCrossover × nPop / 2)
Population size	nPop = 100	Number of mutants	nMutation = round(pMutation × nPop)
Crossover percentage	pCrossover = 0.5	Mutation step size	sigma = 0.1 × (VarMax − VarMin)
Mutation percentage	pMutation = 0.5	Generating reference points	nDivision = 10
			Zr = GenerateReferencePoints(nObj, nDivision);
Mutation rate = 0.02	mu = 0.02	Number of parents (offsprings)	nCrossover = 2 × round(pCrossover × nPop / 2)

Table 3. SPEA/R algorithm parameters.

Maximum number of iterations	10,000	pMutation	1 − pCrossover
Population size	100	nMutation	nPop − nCrossover
Archive size	50	mutation_params.h	0.2
KNN parameter	round(sqrt(nPop + nArchive))	crossover_params.gamma	0.1
pCrossover	0.7	crossover_params.VarMin	VarMin
nCrossover	round(pCrossover × nPop/2) × 2	mutation_params.VarMin	VarMin
mutation_params. VarMax	VarMax	crossover_params.VarMax	VarMax

SPEA/R: Strength Pareto evolutionary algorithm; KNN: k-Recent Neighbor.

Table 4. HNSGA-III& SPEA/R algorithm parameters.

Maximum number of iterations	10,000	pMutation	1 − pCrossover
Population size	100	nMutation	nPop − nCrossover
Archive size	50	mutation_params.h	0.2
KNN Parameter	round(sqrt(nPop + nArchive))	crossover_params.gamma	0.1
pCrossover	0.7	crossover_params.VarMin	VarMin
nCrossover	round(pCrossover × nPop / 2) × 2	mutation_params.VarMin	VarMin
mutation_params.VarMax	VarMax	crossover_params.VarMax	VarMax
Mutation rate	0.02	Mutation step size	0.1 × (VarMax − VarMin)
Number of parents (offsprings)	2 × round(pCrossover × nPop / 2)	Mutation step size	0.1 × (VarMax − VarMin)
Number of mutants	round(pMutation × nPop)		

KNN: k-Recent Neighbor; SPEA/R: Strength Pareto evolutionary algorithm.

Table 5. Results for IGD.

IGD	Average	Median	*SD*	Worst	Best
UF2					
SPEA/R	0.07145	0.04533	0.03754	0.14511	0.03626
NSGA-III	0.12344	0.1252	0.01263	0.14485	0.10454
HNSGA-III&SPEA/R	0.01351	0.01544	0.00255	0.01456	0.01274
UF4					
SPEA/R	0.13433	0.14445	0.00643	0.15454	0.12344
NSGA-III	0.06823	0.06835	0.00254	0.07078	0.06424
HNSGA-III&SPEA/R	0.02645	0.02867	0.00145	0.02734	0.02267
UF5					
SPEA/R	2.50643	2.42532	0.57097	3.03545	1.48643
NSGA-III	1.26765	1.33751	0.13839	1.46735	0.12145
HNSGA-III&SPEA/R	0.47843	0.45451	0.08445	0.53562	0.22371
UF8					
SPEA/R	0.23629	0.43871	0.13765	0.45467	0.24565
NSGA-III	0.56682	0.53666	0.28667	0.69647	0.28530
HNSGA-III&SPEA/R	0.19639	0.27870	0.06766	0.33466	0.17565
UF10					
SPEA/R	1.70325	1.54313	0.55104	3.03813	1.13804
NSGA-III	1.63539	1.59124	0.29349	2.16232	1.22048
HNSGA-III&SPEA/R	1.70346	1.54335	0.55137	3.03836	1.13823

IGD: Inverted Generational Distance; *SD*: standard deviation; SPEA/R: Strength Pareto evolutionary algorithm.
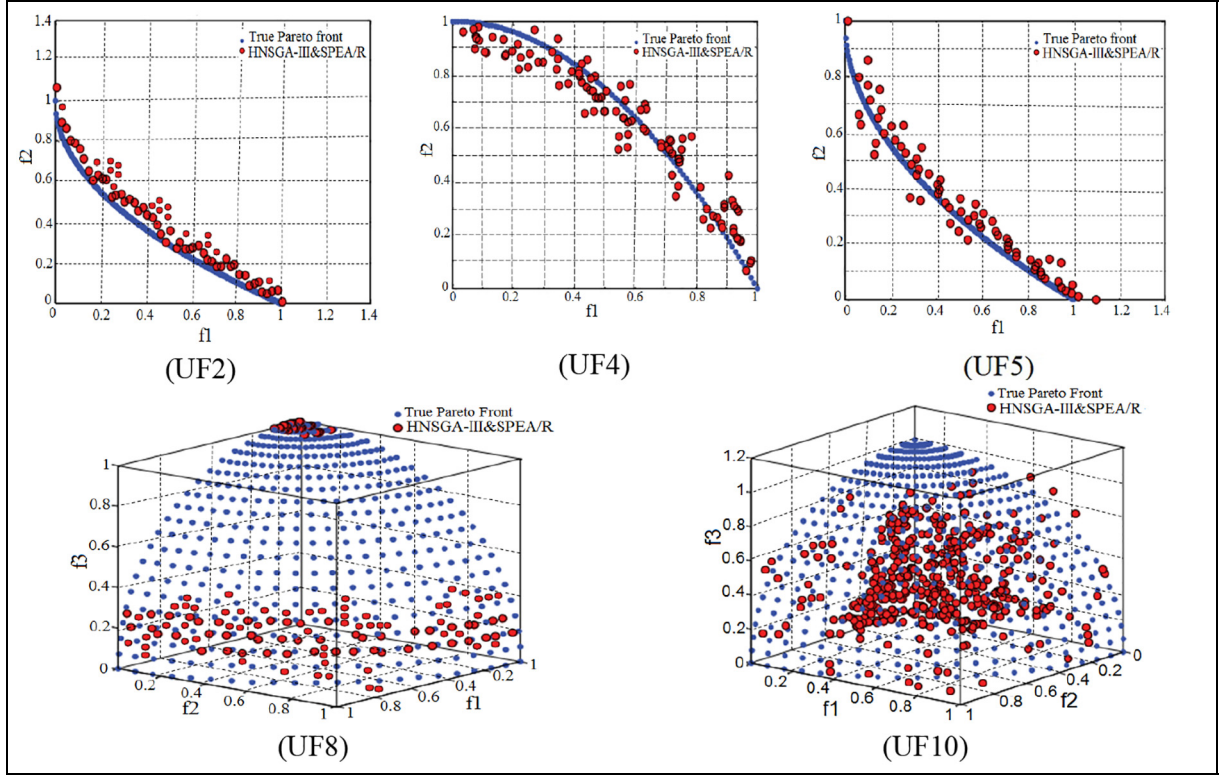
Figure 5. The resulting Pareto-optimal set of HNSGA-III&SPEA/R on each benchmark functions.
SPEA/R: Strength Pareto evolutionary algorithm.

methods because it uses simple operators to create a new population derived from a non-dominant solution.

The hybrid HNSGA-III&SPEA/R method has inherited the advantages of NSGA-III as a reference point based on many-objective NSGA-II, emphasizing that population members are not dominated but close to a set of reference points are provided. And the strengths of SPEA/R are the early resurgence and the expensive computational power of the Pareto-based Evolution algorithm by introducing an effective reference orientation density estimation tool, a new physical assignment scheme, and a new environmental selection strategy, to handle both multi-objective and multiple-objective problems. This hybrid method has yielded a more satisfactory and more accurate result.

Vibration characteristic of the half-car dynamic model

The mounts play an important role in car dynamics system. The principle diagram of the half-car dynamic model with the transmission system is shown in Figure 6.

By using Newton's law, the mathematical model of Figure 6 can be written as below

$$\mathbf{M}\ddot{\mathbf{x}}_{\mathbf{i}} + \mathbf{K}\dot{\mathbf{x}}_{\mathbf{i}} + \mathbf{C}\mathbf{x}_{\mathbf{i}} = \mathbf{Q}(t) \tag{2}$$

where $\mathbf{x}_{\mathbf{i}}$ is Vector-column of displacements and angular oscillations of masses; $\mathbf{M}$ is Matrix of inertial coefficients of car parts; $\mathbf{C}$ is Matrix of coefficients of stiffnesses and torsional rigidity; $\mathbf{K}$ is Matrix of damping coefficients; $\mathbf{Q(t)}$ is Column vector of the perturbing forces and moments; $q_2(t) = q_1(t + \tau)$ with τ: time interval; and va is the vehicle speed

$$\mathbf{Q}(t) = \begin{bmatrix} 2k_1^{\text{IIM}} \cdot \dot{q}_1(t) + 2C_1^{\text{IIM}} \cdot q_1(t), 2k_2^{\text{IIM}} \cdot \dot{q}_2(t) + \\ 2C_2^{\text{IIM}} \cdot q_2(t), 0, 0, P_j(t), P_j(t) \cdot l_{10}, 0, 0, 0, M(t), \\ 0, 0, 0, 0, \gamma \cdot \left[2 \cdot k_1^{\text{IIM}} \cdot \dot{q}_1(t) + 2 \cdot C_1^{\text{IIM}} \cdot q_1(t) \right], \\ \gamma \cdot \left[2 \cdot k_2^{\text{IIM}} \cdot \dot{q}_2(t) + 2 \cdot C_2^{\text{IIM}} \cdot q_2(t) \right], 0, 0, 0 \end{bmatrix}^T \tag{3}$$

$$X = \begin{bmatrix} z_1, z_2, z_0, \varphi_0^{\text{y}}, z_{\text{ca}}, \varphi_{\text{ca}}^{\text{y}}, z_{\text{pk}}, \varphi_{\text{ca}}^{\text{x}}, \varphi_{\text{pk}}^{\text{x}}, \\ \varphi_1, \varphi_2, \varphi_3, \varphi_4, \varphi_5, \varphi_6, \varphi_7, \varphi_8, \varphi_{\prod \text{M}}, \varphi_{3\text{M}} \end{bmatrix}^T \tag{4}$$

Multi-objective optimization functions

There are many indicators to evaluate the vibration of the powertrain. In particular, mean square acceleration (MSA) oscillates at the front and rear of the engine mount, the mean square displacement (MSD) difference between the engine and vehicle chassis at the front and rear engine mount. These are two important parameters that determine the decisive influence of unit engine vibration on chassis. In order to optimally reduce the vibration of the unit engine, we need to simultaneously
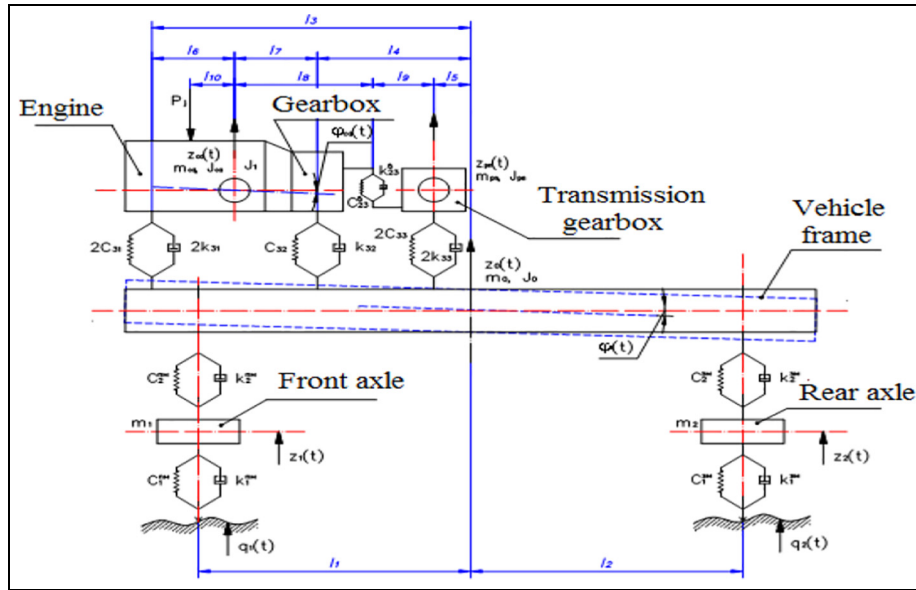
Figure 6. Dynamic vibration model.

optimize the parameters of MSA and MSD at the front and rear of the engine mount.

The average square value of the vibration acceleration of any points can be determined by the formulas

$$\ddot{z}_{ck} = \sqrt{\int_{-\infty}^{\infty} S_{\ddot{z}}(\omega)d\omega} = \sqrt{\int_{-\infty}^{\infty} \omega^4 |W_z(j\omega)|^2 S_q(\omega)} \quad (5)$$

where ω is frequency; $|W_z(j\omega)|^2$ is squared modulus of amplitude and phase characteristics; and $S_q(\omega)$ is spectral density of exposure.

The modules of the amplitude and phase characteristics of the vibratory displacement of the powertrain and the car body in the place of the front mount are

$$W_k^{O_1}(j\omega) = W_0(j\omega) + W_0^{\varphi}(j\omega) \cdot l_3 \quad (6)$$

$$W_{ca}^{O_1}(j\omega) = W_{ca}^{\varphi}(j\omega) + W_{ca}(j\omega) \cdot l_6 \quad (7)$$

where $W_0(j\omega)$ is module amplitude-phase characteristics in the center of the car body; $W_0^{\varphi}(j\omega)$ is module amplitude-phase characteristics of the longitudinal-angular body of the car; $W_k^{O_1}(j\omega)$ is module of the amplitude and phase characteristics of the body in place of the front mount of the powertrain; $W_{ca}(j\omega)$ is module amplitude-phase characteristics in the center of the powertrain of the car; $W_{ca}^{\varphi}(j\omega)$ is module amplitude-phase characteristics of the longitudinal-angular powertrain of the car; and $W_{ca}^{O_1}(j\omega)$ is modulus of amplitude and phase characteristics in place of the front mount of the powertrain.

The modules of the amplitude and phase characteristics of displacement of the engine and the car body in the place of the rear mount are

$$W_k^{O_2}(j\omega) = W_0(j\omega) + W_0^{\varphi}(j\omega) \cdot l_4 \quad (8)$$

$$W_{ca}^{O_2}(j\omega) = W_{ca}(j\omega) - W_{ca}^{\varphi}(j\omega) \cdot l_7 \quad (9)$$

where $W_k^{O_2}(j\omega)$ is the module of the amplitude-phase characteristics of the body in the place of the rear mount of the powertrain and $W_{ca}^{O_2}(j\omega)$ is the module of amplitude and phase characteristics in the place of the rear mount of the powertrain.

The difference of the module frequency response of the vibration of the powertrain and the car body in place of the front mount of the powertrain (C31)

$$W_{ca-k}^{O_1}(j\omega) = W_{ca}^{O_1}(j\omega) - W_k^{O_1}(j\omega) \quad (10)$$

The difference of the frequency response module displacement of the engine and the car body at the rear mount (C32) is

$$W_{ca-k}^{O_2}(j\omega) = W_{ca}^{O_2}(j\omega) - W_k^{O_2}(j\omega) \quad (11)$$

Simulated input parameters

Road surface profiles. When the vehicle moves, there are many factors that cause the vibration, the factors can be listed as the internal force in the car; external forces appear in the process of using acceleration, braking, revolving; exterior conditions such as wind and storm; and boring face street. Among the factors on the bumpy side of the road is the oscillation cause of the vehicle. To simulate the most general calculation, we use the road surface profile as a random function as in Figure 7, and simulated parameters as shown in Table 6–8.
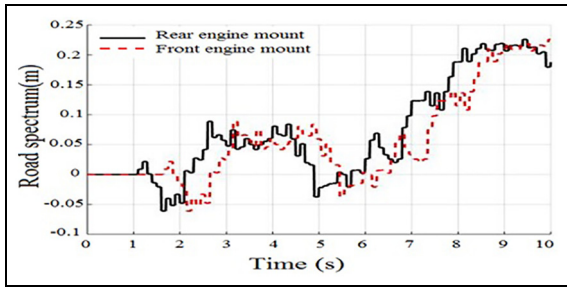
Figure 7. Road surface profiles.

Table 6. Geometric parameters of engine (m).

l_1	l_2	l_3	l_4	l_5
1.225	1.175	1.330	0.520	0.190

l_6	l_7	l_8	l_9	l_{10}
0.187	0.623	0.760	0.210	0.030

Table 7. General settings information.

Mass of the equipped automobile, m_0, kg	1210
Payload, kg	400
The weight of the front wheels, m_1, kg	37
The weight of the rear wheels, m_2, kg	37
The weight of the power unit, m_{ca}, kg	152.2
Transfer case weight, m_{pk}, kg	27.8
Radius crank, r, M	0.04
The ratio of the crank radius to the length of the connecting rod, λ	0.308
Wheel radius in slave mode, r_k, M	0.325

Simulation results of application HNSGA-III&SPEA/R method to optimization of the Powertrain Mount System Stiffness Parameter

Through MATLAB, we calculated four functions of acceleration and displacement according to the stiffnesses of the front and rear engine mount (C31, C32) values as shown in Figure 8.

Table 8. Value ranges of stiffness factor.

Design variables C31, C32	Initial values	Varying ranges	
		Lower	Upper
Stiffnesses of rear engine mount C31 (N/m)	690,000	100,000	900,000
Stiffnesses of front engine mount C32 (N/m)	190,000	100,000	900,000

The results of multi-objective optimization would be a set of non-dominated optimized points, it is called the Pareto set. These points offer a wide range of parameters to the designer to choose the optimum point depending on his designing conditions. There are always conflicting objective functions in vehicle designing where improvement in one function may have an unfavorable influence on other functions. In this article, multi-objective optimization for all four-objective functions is done simultaneously. By application of HNSGA-III&SPEA/R optimization algorithm, we obtain results as shown in Figures 9–11. Area A is Global Pareto front of the mount system as shown in Figure 11.

The average square of the Pareto front of MSD at the front engine mount: f1 = 2.1773e-04 (m).

The average square of the Pareto front of MSA at the front engine mount: f2 = 13.8276 (m/s²).

The average square of the Pareto front of MSD at the rear engine mount: f3 = 4.0500e-04 (m).

The average square of the Pareto front of MSA at the rear engine mount: f4 = 18.1001 (m/s²).

Figure 9 depicts a set of Pareto front sets after 10,000 repetitions with an initial population of 100. This figure shows the optimal points of the Pareto front set according to the coordinate axis of the displacement and acceleration functions of the two mount.

Figure 10 shows the optimal Pareto front points on the displacement surface and the acceleration surface of two engine mounts. From here, there is a visual view of the optimal points corresponding to the hardness of C31 and C32.
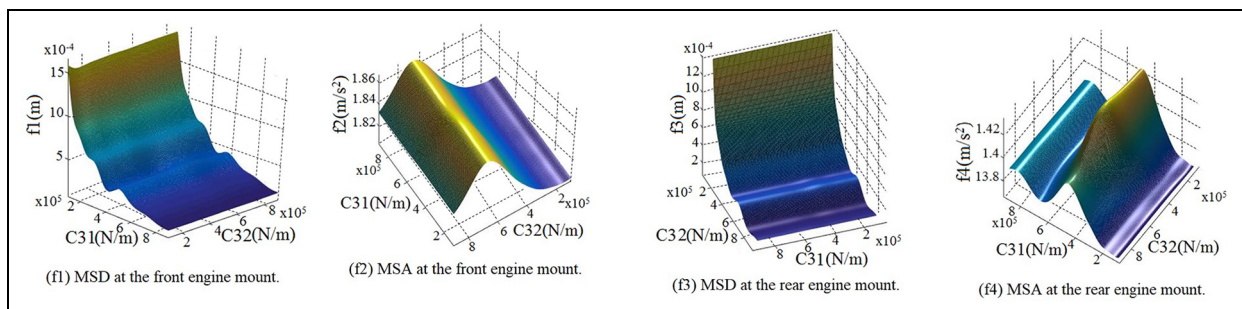

Figure 8. Values of four-objective optimization functions: (f1) MSD at the front engine mount, (f2) MSA at the front engine mount, (f3) MSD at the rear engine mount, and (f4) MSA at the rear engine mount.
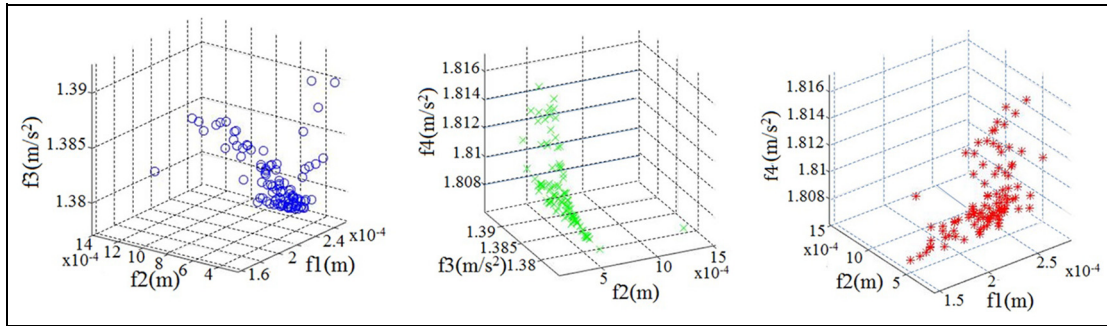MSD: mean square displacement; MSA: mean square acceleration.

Figure 9. Pareto front of the solutions after 1000 generations, 200 population.

(f1) Pareto front of MSD at the front engine mount.

(f2) Pareto front of MSA at the front engine mount.

(f3) Pareto front of MSD at the rear engine mount.
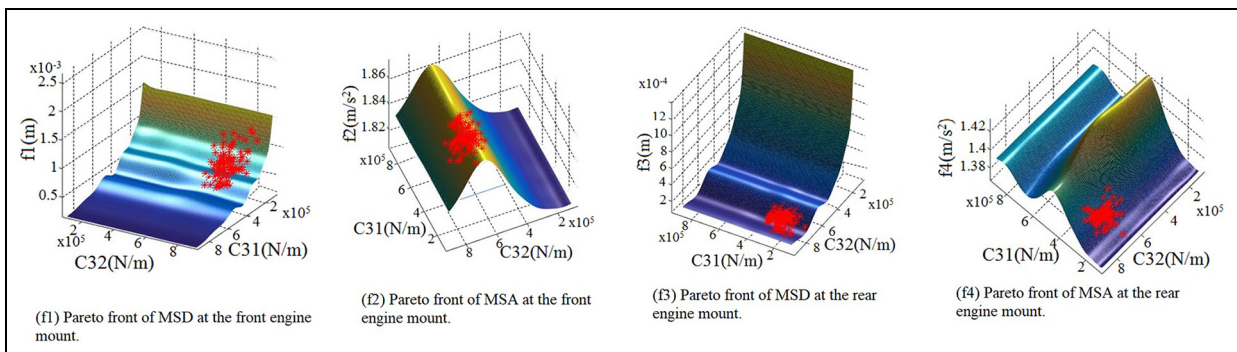
(f4) Pareto front of MSA at the rear engine mount.

Figure 10. Global Pareto front of four-Optimization Objective: (f1) Pareto front of MSD at the front engine mount, (f2) Pareto front of MSA at the front engine mount, (f3) Pareto front of MSD at the rear engine mount, and (f4) Pareto front of MSA at the rear engine mount.
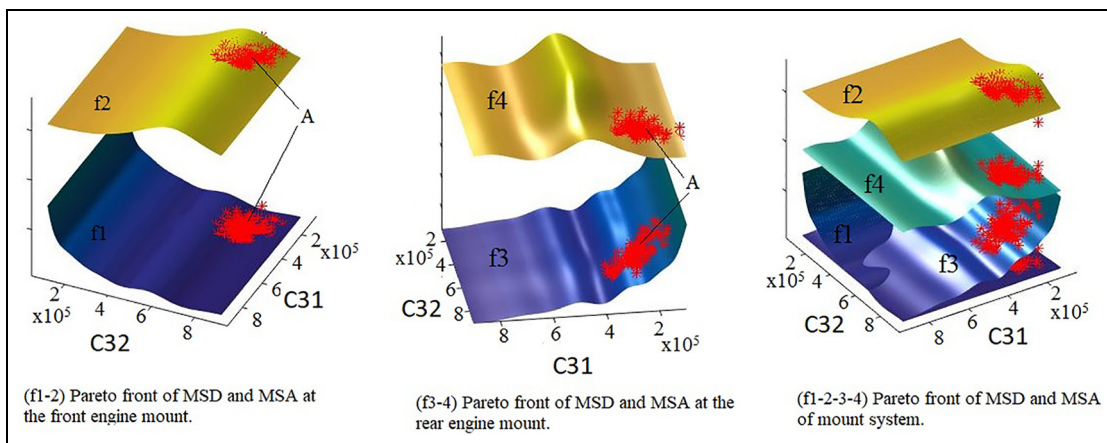MSD: mean square displacement; MSA: mean square acceleration.

(f1-2) Pareto front of MSD and MSA at the front engine mount.

(f3-4) Pareto front of MSD and MSA at the rear engine mount.

(f1-2-3-4) Pareto front of MSD and MSA of mount system.

Figure 11. Global Pareto front of the mount system: (f1–f2) Pareto front of MSD and MSA at the front engine mount, (f3–f4) Pareto front of MSD and MSA at the rear engine mount, and (f1–f4) Pareto front of MSD and MSA of mount system.
MSD: mean square displacement; MSA: mean square acceleration.

Figures 10 and 11 visually depict the optimal points according to the hardnesses of C31 and C32, respectively, according to displacement and acceleration in each mount and in both vehicles in the half-car simulation model. From here, depending on the different design requirements, the designer chooses which optimal point best fits the design requirement. Table 9 is

the simulation results of optimization of the Powertrain Mount System Stiffness Parameter.

Conclusion

The combination of the SPEA/R algorithm and the GA NSGA-III has been implemented in this paper. This

Table 9. Result of Pareto-optimal front of powertrain mount system stiffness parameter.

C31 (N/m)	C32 (N/m)	C31 (N/m)	C32 (N/m)	Iteration times
215,318	847,090	349,070	857,041	7905
224,335	780,010	354,053	789,030	
247,505	861,142	355,258	866,140	
257,400	887,160	358,467	871,144	
260,026	875,149	360,279	874,132	
290,511	826,550	364,260	816,440	
315,018	877,167	365,955	841,051	
318,906	835,233	368,550	831,210	
320,050	876,646	374,266	881,052	
330,430	766,060	375,011	886,102	
345,647	810,041	375,298	856,035	

Figure 13. Displacement of the vehicle frame.
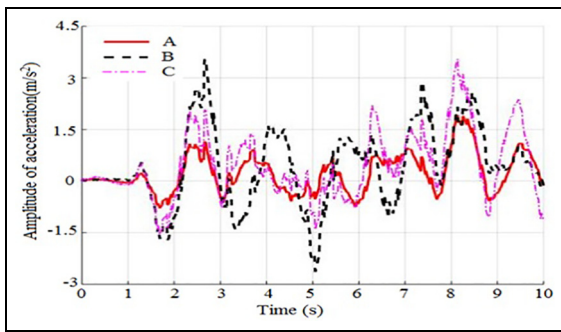
Figure 12. Acceleration of the vehicle frame.

technique results in the globally optimal set of multi-object problems. Hybrid method HNSGA-III&SPEA/R has been rated as high performance. This has been assessed through a series of comparative testing methods for benchmarking functions two goals and three goals. In addition, these results are compared with other multi-purpose optimization methods such as SPEA/R and NSGA-III. The numerical results demonstrate that this new hybrid algorithm is more effective in solving multi-objective optimization problems with many possibilities for convergence and search.

HNSGA-III&SPEA/R has been applied in the problem of Powertrain mount system stiffness parameters optimization. Simulation results comparing one of the results in the set of the Pareto front from the HNSGA-III&SPEA/R algorithm with different stiffness values (C31, C32) are shown in Figures 12 and 13.

Figure 12 shows the acceleration of the vehicle frame corresponding to the different stiffness values. Symbol A corresponds to the optimal stiffness value in a set of the Pareto front. Symbol B corresponds to C31 = 290,000; C32 = 350,000. Symbol C corresponds to C31 = 790,000; C32 = 750,000. From the graph, we see that the smallest acceleration is at the optimal stiffness value. Similarly, Figure 13 shows the displacement of the vehicle frame corresponding to the different stiffness values. Symbol A corresponds to the optimal
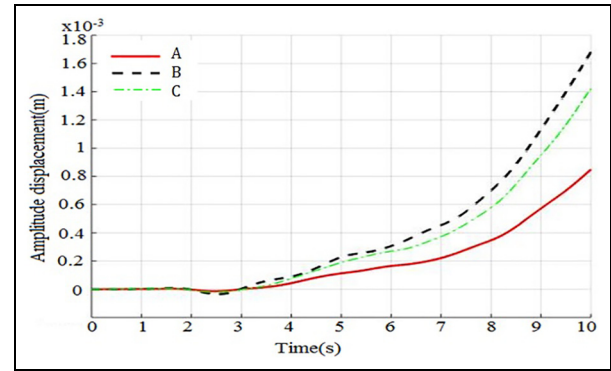
stiffness value in a set of the Pareto front. Symbol B corresponds to C31 = 290,000; C32 = 350,000. Symbol C corresponds to C31 = 790,000; C32 = 750,000. From the graph, we see that the smallest displacement is at the optimal stiffness value.

Declaration of conflicting interests

Funding

ORCID iD

Dinh-Nam Dao [iD] https://orcid.org/0000-0001-9810-2096

References

1. Yu YH, Naganathan NG and Rao VD. A literature review of automotive vehicle engine mounting systems. *Mech Mach Theory* 2001; 36: 123–142.
2. Adiguna H, Tiwari M, Singh R, et al. Transient response of a hydraulic engine mount. *J Sound Vib* 2003; 268: 217–248.
3. Xiong F, Wang D, Wang D, et al. Lightweight optimization of the front end structure of an automobile body using entropy-based grey relational analysis. *Proc IMechE, Part D: J Automobile Engineering* 2019; 233: 917–934.
4. Konak A, Coit D and Smith E. Multi-objective optimization using genetic algorithms: a tutorial. *Reliab Eng Syst Safe* 2006; 91: 92–107.
5. Deb K, Pratap A, Agarwal S, et al. A fast elitist multiobjective genetic algorithm: NSGA-II. *IEEE T Evolut Comput* 2002; 6: 182–197.
6. Chang LC and Chang FJ. Multi-objective evolutionary algorithm for operating parallel reservoir system. *J Hydrol* 2009; 377: 12–20.

7. Ishibuchi H, Tsukamoto N and Nojima Y. Evolutionary many-objective optimization: a short review. In: *Proceedings of IEEE congress on evolutionary computation*, Hong Kong, China, 1–6 June 2008. New York: IEEE.

8. Malekmohammadi B, Zahraie B and Kerachian R. A ranking solution of multi-objective reservoir operation optimization models using multi-criteria decision analysis. *Expert Syst Appl* 2011; 38: 7851–7863.

9. Kalyanmoy D and Jain H. Handling many-objective problems using an improved NSGA-II procedure. In: *CEC 2012: Proceedings of IEEE congress on evolutionary computation*, Brisbane, QLD, Australia, 10–15 June 2012. New York: IEEE.

10. Deb K and Jain H. An evolutionary many objective optimization algorithms using reference-point based non-dominated sorting approach, part I: solving problems with box constraints. *IEEE Trans Evol Comput* 2014; 18: 577–601.

11. Kim M, Hiroyasu T, Miki M, et al. SPEA2 + : improving the performance of the strength Pareto evolutionary algorithm 2. In: Yao X, Burke EK, Lozano JA, et al. (eds) *Parallel problem solving from nature—PPSN VIII (Lecture Notes in Computer Science)*, vol. 3242. Berlin; Heidelberg: Springer, 2004, pp.742–751.

12. Zitzler E, Laumanns M and Thiele L. Evolutionary methods for design optimization and control with applications to industrial problems. In: *Proceedings of the EUROGEN2001 conference*, Athens, 19–21 September 2001, pp.95–100. Barcelona: International Center for Numerical Methods in Engineering.

13. Borisevic J and Bartlett LM. Safety system optimization by improved strength Pareto evolutionary approach (SPEA2). In: *Proceedings of the 17th advances in reliability technology symposium (ARTS)*, Loughborough, 17–19 April 2007, pp.38–49. Loughborough: Loughborough University.

14. Mori H and Kakuta H. Modified SPEA2 for probabilistic reliability assessment in smart grids. *Procedia Comp Sci* 2011; 6: 435–440.

15. De Tommasi L, Beelen TGJ, Sevat MF, et al. *Multi-objective optimization of RF circuit blocks via surrogate models and NBI and SPEA2 methods (CASA-report)*, vol. 1132. Eindhoven: Technische Universiteit Eindhoven, 2011.

16. Sofianopoulos S and Tambouratzis G. Studying the SPEA2 algorithm for optimising a pattern-recognition based machine translation system. In: *Proceedings of the 2011 IEEE symposium on computational intelligence in multicriteria decision-making (MCDM2011)*, Paris, 11–15 April 2011, pp.97–104. New York: IEEE.

17. Zhao F, Lei W, Ma W, et al. An improved SPEA2 algorithm with adaptive selection of evolutionary operators scheme for multiobjective optimization problems. *Math Probl Eng* 2016; 2016: 8010346.

18. Hamida IB, Salah SB, Msahli F, et al. Strength pareto evolutionary algorithm 2 for environmental/economic power dispatch. In: *ICMIC 2015: 7th international conference on modelling, identification, and control*, Sousse, Tunisia, 18–20 December. New York: IEEE.

19. Jiang S and Yang S. A strength pareto evolutionary algorithm based on reference direction for multiobjective and many-objective optimization. *IEEE* T Evolut Comput 2017; 21: 329–346.

20. Mirjalili S, Saremi S, Mirjalili SM, et al. Multi-objective grey wolf optimizer: a novel algorithm for multi-criterion optimization. *Expert Syst Appl* 2016; 47: 106–119.

21. Premalatha K and Natarajan AM. Hybrid PSO and GA for global maximization. *Int J Open Problems Comp Math* 2009; 2: 597–608.

22. Velazquez OJ, Coello CC and Arias-Montano A. Multi-objective compact differential evolution. In: *2014 IEEE symposium on differential evolution (SDE)*, Orlando, FL, 9–12 December 2014, pp.1–8. New York: IEEE.

23. Hemmatian H, Fereidoon A and Assareh E. Optimization of hybrid laminated composites using the multi-objective gravitational search algorithm (MOGSA). *Eng Optim* 2014; 46: 1169–1182.

24. Shi X and Kong D. A multi-objective ant colony optimization algorithm based on elitist selection strategy. *Metall Min Indus* 2015; 7: 333–338.

25. Hancer E, Xue B, Zhang M, et al. A multi-objective artificial bee colony approach to feature selection using fuzzy mutual information. In: *2015 IEEE congress on evolutionary computation (CEC)*, Sendai, Japan, 25–28 May 2015, pp.2420–2427. New York: IEEE.

26. Lin W, Yu DY, Zhang C, et al. A multi-objective teaching-learning-based optimization algorithm to scheduling in turning processes for minimizing makespan and carbon footprint. *J Clean Prod* 2015; 101: 337–347.

27. Pradhan PM and Panda G. Solving multi-objective problems using cat swarm optimization. *Expert Syst Appl* 2012; 39: 2956–2964.

28. Jeong S, Hasegawa S, Shimoyama K, et al. Development, and investigation of efficient GA/PSO-hybrid algorithm applicable to real-world design optimization. In: *2009 IEEE congress on evolutionary computation*, Trondheim, 18–21 May 2009. New York: IEEE.

29. Bai H. An improved multi-objective particle swarm optimization. *Int J Comput Optim* 2016; 3: 105–120.

30. Pourtakdoust SH and Zandavi SM. A hybrid simplex non-dominated sorting genetic algorithm for multiobjective optimization. *Int J Swarm Intel Evol Comput* 2016; 5: 3.

31. Yang G, Xu T, Li X, et al. An efficient hybrid algorithm for multiobjective optimization problems with upper and lower bounds in engineering. *Math Probl Eng* 2015; 2015: 932029.

32. Rashidi E, Jahandar M and Zandieh M. An improved hybrid multi-objective parallel genetic algorithm for hybrid flow shop scheduling with unrelated parallel machines. *Int J Adv Manuf Tech* 2010; 49: 1129–1139.

33. Zhang Q, Zhou A and Zhao S. *Multi-objective optimization test instances for the CEC 2009 special session and competition*. Essex: University of Essex, 2008, pp.1–30.

34. Schott JR. *Fault tolerant design using single and multicriteria genetic algorithm optimization*. MS Thesis, Department of Aeronautics and Astronautics, Massachusetts Institute of Technology, Includes bibliographical references, 1995, pp.199–200, http://hdl.handle.net/1721.1/11582